

3.6 Migration with velocity estimation (revised lecture notes)

Jon F. Claerbout

In preparing my new book I discovered a surprising relationship between Hale's constant offset dip moveout filters, and the radial trace approach of Rick Ottolini. You may wish to skip over the early parts of this section to the new material near the end.

3.6 Migration with Velocity Estimation

We often face the three complications dip, offset, and unknown velocity at the same time. The double-square-root equation provides an attractive avenue when the velocity is known, but when it isn't, we are left with velocity-estimation procedures, such as that in the last section, *which assume no dip*. In this section a means will be developed of estimating velocity in the presence of dip.

Dip Moveout — Sherwood's Devilish

Recall (Section 3.2) Levin's expression for the travel time of the reflection from a bed dipping at angle α from the horizontal:

$$t^2 v^2 = 4(y - y_0)^2 \sin^2 \alpha + 4h^2 \cos^2 \alpha \quad (1)$$

In (h, t) -space this curve is a hyperbola. Scaling the velocity by $\cos \alpha$ makes the travel-time curve identical to the travel-time curve of the dip-free case. This is the conventional approach to stacking and velocity analysis. It is often satisfactory. Sometimes it is unsatisfactory because the dip angle is not a single-valued function of space. For example, near a fault plane there will be diffractions. They are a superposition of all dips, each usually being weaker than the reflections. Many dips are present in the same place. They blur the velocity estimate and the stack.

In principle, migration before stack — some kind of implementation of the full DSR equation — solves this general problem. But where do we get the velocity to use in the migration equations? Although migration is somewhat insensitive to velocity when only small angles are involved, migration becomes sensitive to velocity when wide angles are involved.

The migration process should be thought of as being interwoven with the velocity estimation process. J.W.C. Sherwood (1976) showed how the two processes, migration and velocity estimation, should be interwoven. The moveout correction should be considered in two parts, one depending on offset, the NMO, and the other depending on dip. This latter process was conceptually new. Sherwood described the process as a kind of filtering, but he did not provide implementation details. He called his process *Devilish*, an acronym for "dipping-event velocity inequalities licked". The process was later described more functionally by Yilmaz as *pre-stack partial migration*, but the process has finally come to be called simply *dip moveout* (DMO). We will first see Sherwood's results, then Rocca's conceptual model of the DMO process, and

finally two conceptually-distinct, quantitative specifications of the process.

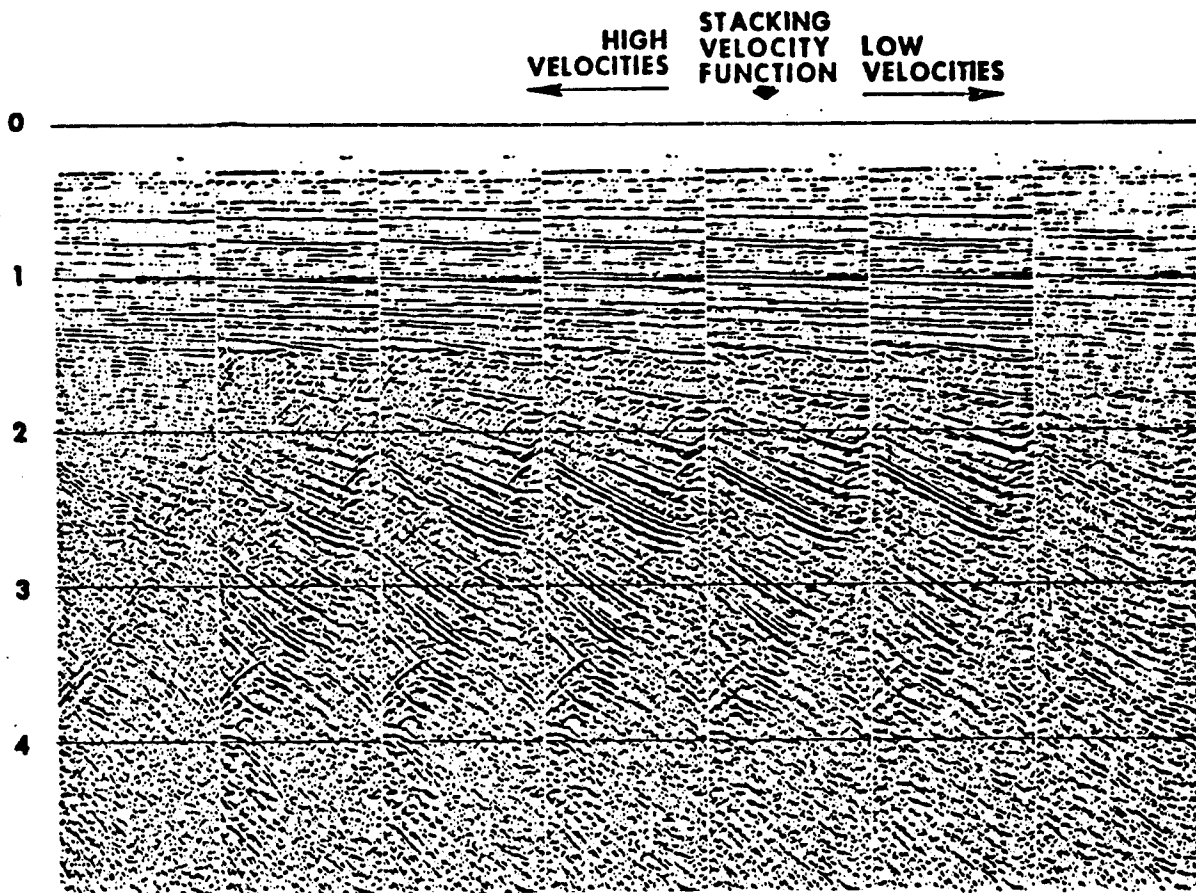


FIG. 1. Conventional stacks with varying velocity. (distributed by Digicon, Inc.)

Figure 1 contains a panel from a stacked section. The panel is shown several times; each time the stacking velocity is different. It should be noted that at the low velocities, the horizontal events dominate, whereas at the high velocities, the steeply dipping events dominate. After the *Devilish* correction was applied, the data was restacked as before. Figure 2 shows that the stacking velocity no longer depends on the dip. This means that after *Devilish*, the velocity may be determined without regard to dip. In other words, events with all dips contribute to the same consistent velocity rather than each dipping event predicting a different velocity. So the *Devilish* process should provide better velocities for data with conflicting dips. And we can expect a better final stack as well.

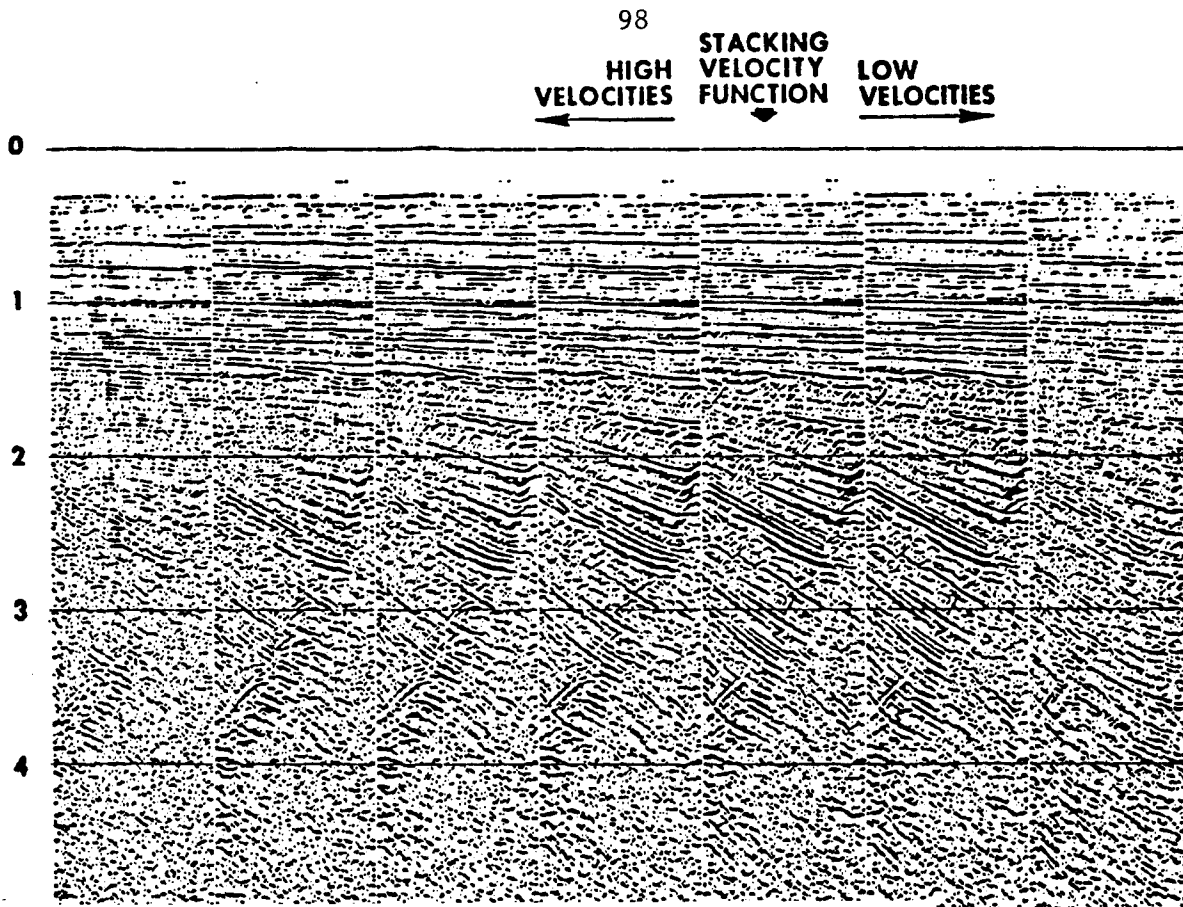


FIG. 2. *Devilish* stacks with varying velocity. (distributed by Digi-con, Inc.)

Rocca's Smear Operator

Fabio Rocca developed a clear conceptual model for Sherwood's dip corrections. Figure 3 illustrates Rocca's concept of a prestack partial-migration operator. Imagine a constant-offset section $P(t, y, h=h_0)$ containing an impulse function at some particular (t_0, y_0) . The earth model implied by this data is a reflector shaped like an ellipse, with the shot point at one focus and the receiver at the other. Starting from this earth model, a zero-offset section is made by forward modeling — that is, each point on the ellipse is expanded into a hyperbola. Combining the two operations — constant-offset migration and zero-offset diffraction — gives the Rocca operator.

The Rocca operator is the curve of osculation in figure 3, i.e. the smile-shaped curve where the hyperbolas reinforce one another. If the hyperbolas in figure 3 had been placed everywhere on the ellipse instead of at isolated points, then the osculation curve would be the only thing visible (and you wouldn't be able to see where it came from).

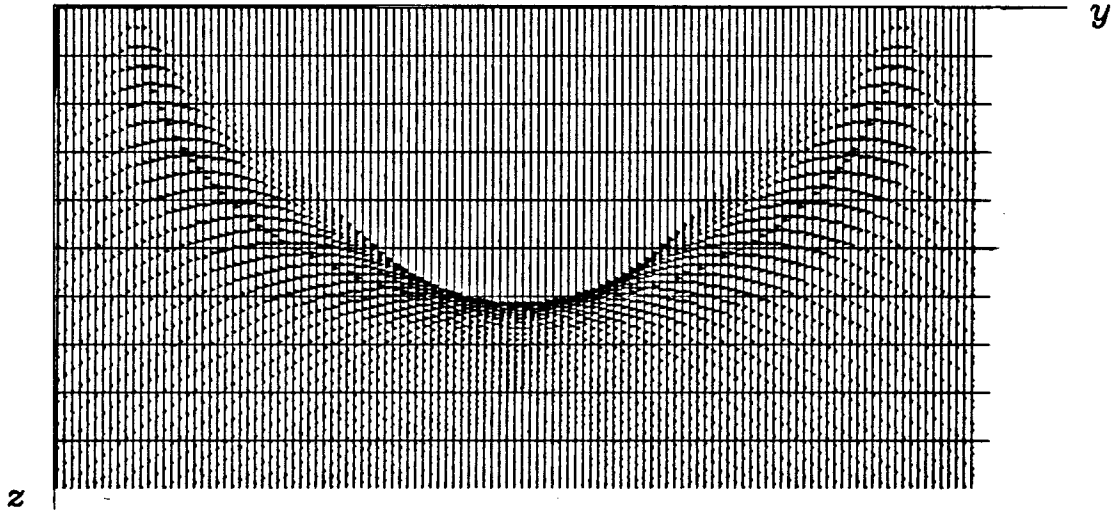


FIG. 3. Rocca's prestack partial-migration operator is a superposition of hyperbolas, each with its top on an ellipse. Convolution (over midpoint) Rocca's operator onto a constant-offset section converts it to a zero-offset section. (Gonzalez)

The analytic expression for the travel time on the Rocca smile is the end of a narrow ellipse, shown in figure 4. We will omit the derivation of the equation for this curve which turns out to be

$$1 = \frac{(y - y_0)^2}{h^2} + \frac{t^2}{t_0^2} \quad (2)$$

The Rocca operator appears to be velocity independent, but it is not completely so because the curve cuts off at $dt/dy = 2/v$.

The Rocca operator transforms a constant-offset section into a zero-offset section. This transformation achieves two objectives: first, it does normal-moveout correction; second, it does Sherwood's dip corrections. The operator of figure 3 is convolved across the midpoint axis of the constant-offset section, giving as output a zero-offset section at just one time, say, t_0 . For each t_0 a different Rocca operator must be designed. The outputs for all t_0 values must be superposed. Figure 5 shows a superposition of several Rocca smiles for several values of t_0 .

This operator is particularly attractive from a practical point of view. Instead of using a big, wide ellipse and doing the big job of migrating each constant-offset section, only the narrow, little Rocca operator is needed. From figure 5 we see that the energy in the dip moveout operator concentrates narrowly near the bottom. In the limiting case that h/vt_0 is small, the energy does all go to

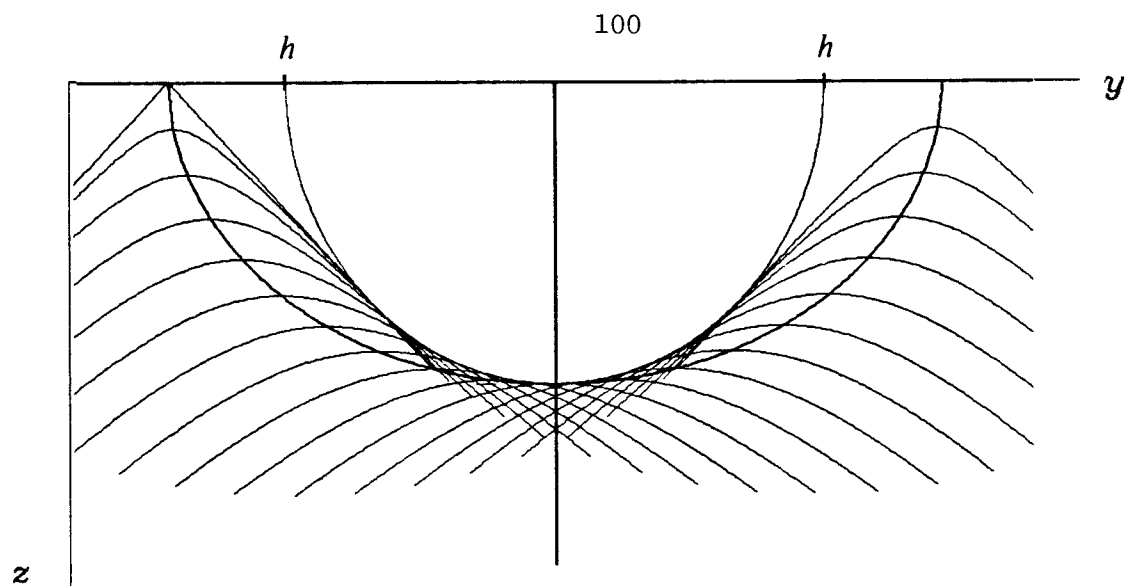


FIG. 4. Rocca's smile. (Ronen)

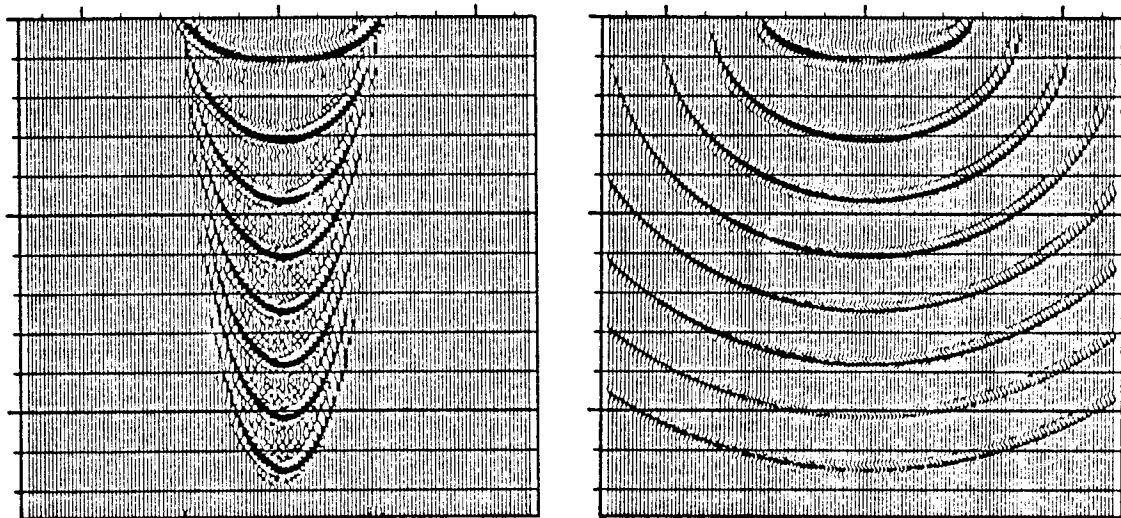


FIG. 5. Point response of of dip moveout (left) compared to constant-offset migration (right). (Hale)

the bottom. When all the energy is concentrated near the bottom point, the Rocca operator is effectively a delta function. After compensating each offset to zero offset, velocity is determined by the normal-moveout residual; then data is stacked and migrated.

The *narrowness* of the Rocca ellipsoid is an advantage in two senses. Practically, it means that not many midpoints need to be brought into the computer main memory before velocity estimation and stacking are done. More fundamentally, since the operator is so compact, it does not do a lot to the data. This is

important because the operation is done at an early stage, before the velocity is well known. So it may be satisfactory to choose the velocity for the Rocca operator as a constant, regional value, say, 2.5 km/sec.

An expression for the travel-time curve of the dip moveout operator might be helpful for Kirchhoff-style implementations. More to the point is a Fourier representation for the operator itself which we will find next.

Hale's Constant-Offset Dip Moveout

Hale (1983) found a Fourier representation of dip moveout. Refer to the defining equations in table 1.

NMO	$t \rightarrow t_n$	$t = \sqrt{t_n^2 + 4h^2v^{-2}}$
Levin's NMO	$t \rightarrow t_0$	$t = \sqrt{t_0^2 + 4h^2v^{-2}\cos^2\alpha}$
DMO	$t_n \rightarrow t_0$	$t_n = \sqrt{t_0^2 - 4h^2v^{-2}\sin^2\alpha}$

TABLE 1. Equations for normal moveout and dip moveout. Substituting the DMO equation into the NMO equation yields Levin's dip corrected NMO.

To use the dip dependent equations in table 1, it is necessary to know the earth dip α . The dip can be measured from a zero-offset section. On the zero-offset section in Fourier space, the sine of the dip is $v k_y / 2\omega$. To stress that this measurement applies only on the *zero*-offset section, we shall always write ω_0 .

$$\sin \alpha = \frac{v k_y}{2 \omega_0} \quad (3)$$

In the absence of dip, NMO should convert any trace into a replica of the zero-offset trace. Likewise in the presence of dip, the combination of NMO and DMO should convert any constant-offset section to a zero-offset section. Pseudo-zero-offset sections manufactured in this way from constant-offset sections will be

denoted by $p_0(t_0, h, y)$. First take the midpoint coordinate y over to its Fourier dual k_y . Then take the Fourier transform over time.

$$P_0(\omega_0, h, k_y) = \int dt_0 e^{i\omega_0 t_0} P_0(t_0, h, k_y) \quad (4)$$

Change the variable of integration from t_0 to t_n .

$$P_0(\omega_0, h, k_y) = \int dt_n \frac{dt_0}{dt_n} e^{i\omega_0 t_0(t_n)} P_0(t_0(t_n), h, k_y) \quad (5)$$

Express the integrand in terms of NMOed data P_n . This is done by means of $P_n(t_n, h, k_y) = P_0(t_0(t_n), h, k_y)$.

$$P_0(\omega_0, h, k_y) = \int dt_n \frac{dt_0}{dt_n} e^{i\omega_0 t_0(t_n)} P_n(t_n, h, k_y) \quad (6)$$

As with Stolt migration, the Jacobian of the transformation, dt_0/dt_n scales things but doesn't do time shifts. The DMO is really done by the exponential term.

Omitting the Jacobian (which does little) the over-all process may be envisioned with the program outline:

```

P(ky) = FT[P(y)]
Pn(tn) = NMO[P(t)]
for all ky {      # three nested loops, interchangeable
for all h {      # three nested loops, interchangeable
for all ω0 {      # three nested loops, interchangeable
    sum = 0
    for all tn {
        sum = sum + exp[ iω0 [ tn2 +  $\frac{h^2 k_y^2}{\omega_0^2}$  ]1/2 ] Pn(tn, h, ky)
    }
    P0(ω0, h, ky) = sum
} } }
p0(t0, h, y) = FT2D[P0(ω0, h, ky)]

```

Notice that the exponential in the inner loop in the program does not depend on velocity. The velocity in the DMO equation in table 1 disappears on substitution of $\sin \alpha$ from equation (3). So dip moveout does not depend on velocity.

The procedure outlined above requires NMO before DMO. To reverse the order would be an approximation. This is unfortunate because we would prefer to do the costly, velocity-independent DMO step once, before the iterative, velocity-estimating NMO step.

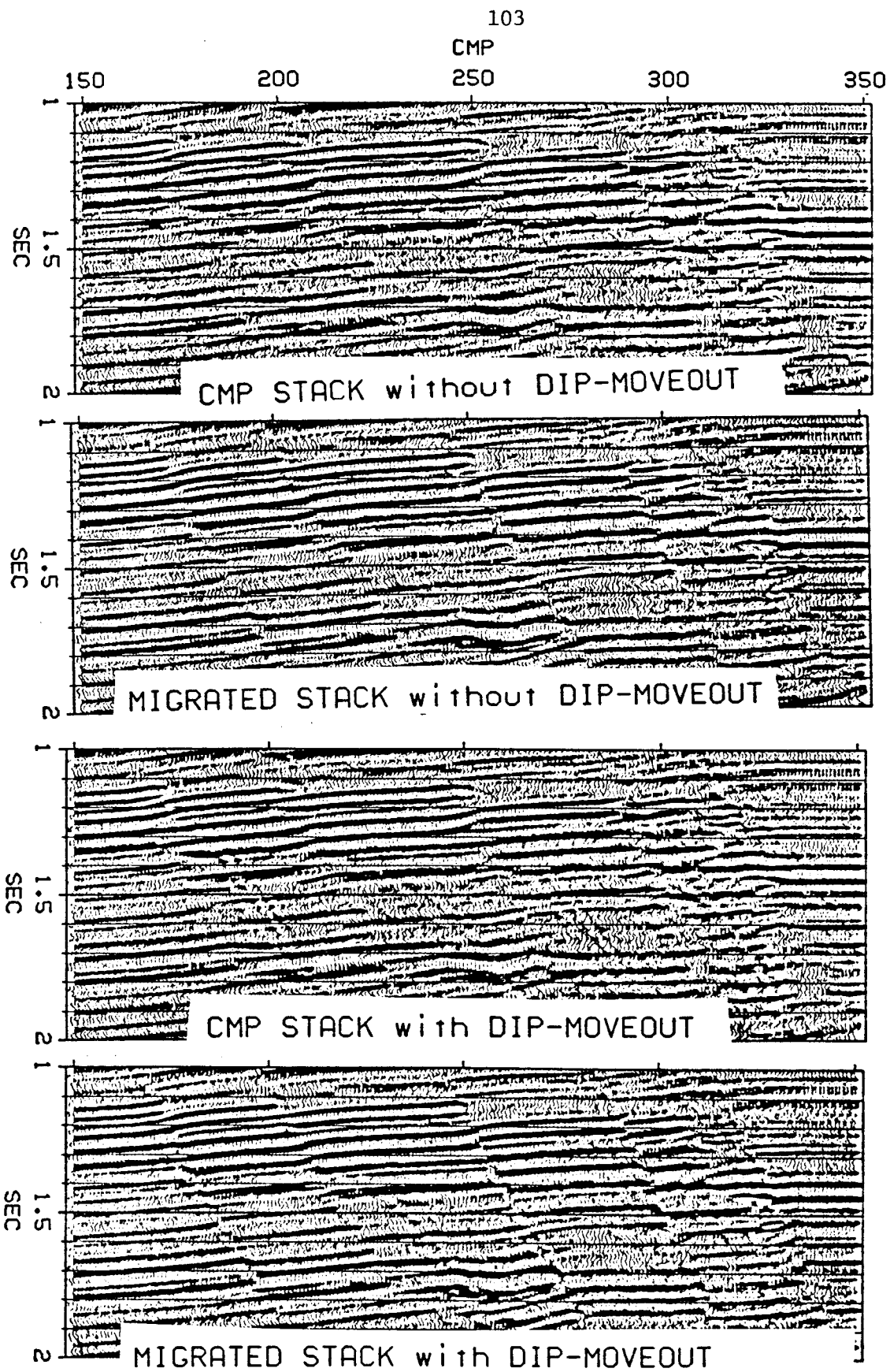


FIG. 6. Processing with dip moveout (Hale, 1983)

Ottolini's Radial Traces

Ordinarily we regard a common-midpoint gather as a collection of seismic traces, that is, a collection of time functions, each one for some particular offset h . But this (h, t) data space could be represented in a different coordinate system. A system with some nice attributes is the radial-trace system introduced by Turhan Taner. In this system the traces are not taken at constant h , but at constant angle. The idea is illustrated in figure 7.

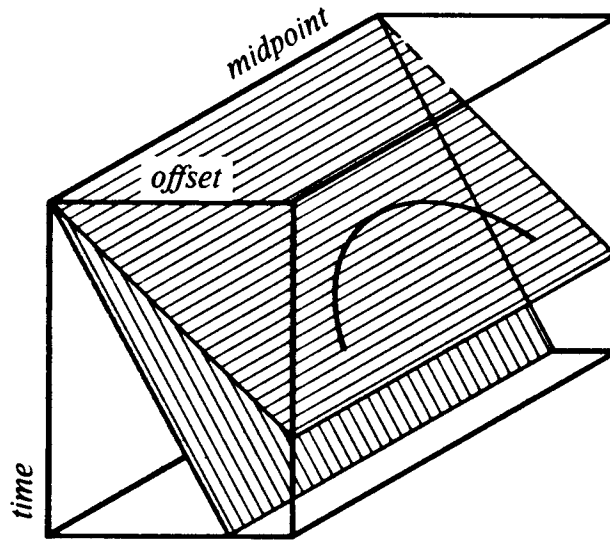


FIG. 7. Inside the data volume of a reflection seismic traverse are planes called *radial-trace sections*. A point scatterer inside the earth puts a hyperbola on a radial-trace section.

Besides having some theoretical advantages, which will become apparent, this system also has some practical advantages, notably: (1) the traces neatly fill the space where data are nonzero; (2) the traces are close together at early times where wavelengths are short, and wider apart where wavelengths are long; and (3) the energy on a given trace tends to represent wave propagation at a fixed angle. The last characteristic is especially important with multiple reflections. But for our purposes the best attribute of radial traces is still another one.

Richard Ottolini noticed that a point scatterer in the earth appears on a radial-trace section as an *exact* hyperbola, not a flat-topped hyperboloid. The travel-time curve for a point scatterer, Cheops' pyramid, can be written as a "string length" equation, or a stretched-circle equation (Section 3.2). Making the definition

$$\sin \psi = \frac{2h}{vt} \quad (7)$$

and substituting into Section 3.2, equation (13) yields

$$vt = 2 \left[\frac{z^2}{\cos^2 \psi} + (y - y_0)^2 \right]^{1/2} \quad (8)$$

Scaling the z -axis by $\cos \psi$ gives the circle and hyperbola case all over again! The hidden hyperbola is shown as a three-dimensional sketch in figure 8.

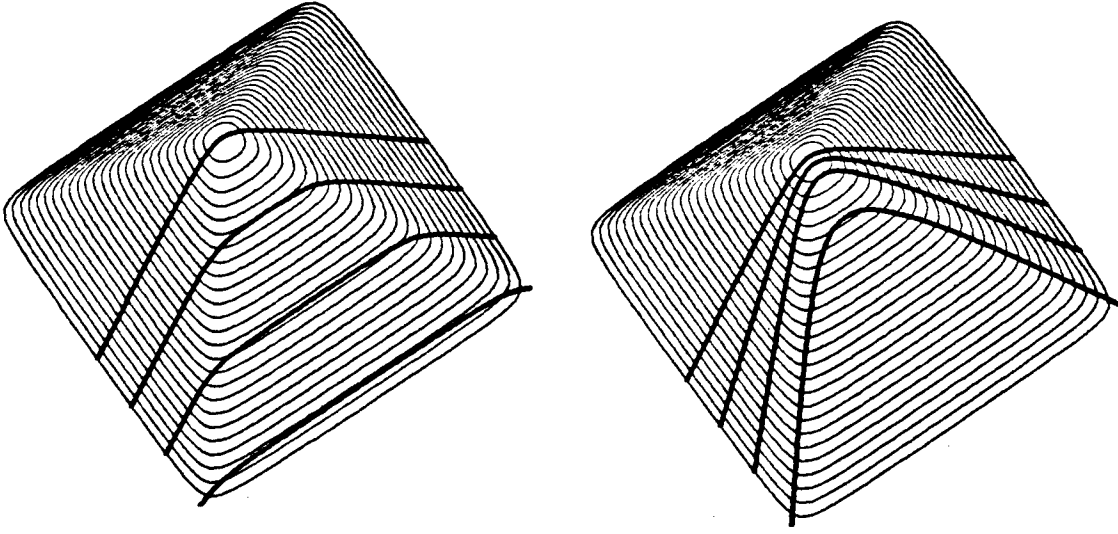


FIG. 8. An unexpected hyperbola in Cheops' pyramid is the diffraction hyperbola on a radial-trace section. (Ottolini)

We will see that the radial hyperbola of figure 8 is easier to handle than the flat-topped hyperboloid that is seen at constant h . Refer to the equations in table 2.

The second equation in table 2 is the usual exploding reflector equation for zero-offset migration. It may also be obtained from the DSR by setting $H = 0$. As written it contains the earth velocity, not the half velocity. Recall Ottolini's result that hyperbolas of differing ψ values are related to one another by scaling the z -axis by $\cos \psi$. According to Fourier transform theory, scaling z by a $\cos \psi$ divisor will scale k_z by a $\cos \psi$ multiplier. This means that the first equation in the table can be used for migrating and diffracting hyperbolas on radial trace sections. Eliminating k_z from the first and second equations yields the middle equation $\omega \rightarrow \omega_0$ in table 2. This middle equation combines the operation of

migration	$\omega \rightarrow k_z$	$k_y^2 + k_z^2 \cos^2 \psi = 4\omega^2 / v^2$
zero-offset diff.	$k_z \rightarrow \omega_0$	$k_y^2 + k_z^2 = 4\omega_0^2 / v^2$
DMO+NMO	$\omega \rightarrow \omega_0$	$.25v^2 k_y^2 \sin^2 \psi + \omega_0^2 \cos^2 \psi = \omega^2$
radial DMO	$\omega \rightarrow \omega_s$	$.25v^2 k_y^2 \sin^2 \psi + \omega_s^2 = \omega^2$
radial NMO	$\omega_s \rightarrow \omega_0$	$\omega_0 \cos \psi = \omega_s$

TABLE 2. Equations defining dip moveout in radial trace coordinates and also ordinary moveout in radial trace coordinates.

migrating all offsets (really any radial angle) and then diffracting out to zero offset. Thus the total effect is that of *offset continuation*, i.e. NMO and DMO. The last two equations in table 2 are a decomposition of the the middle equation $\omega \rightarrow \omega_0$ into two sequential processes, $\omega \rightarrow \omega_s$ and $\omega_s \rightarrow \omega_0$. These two processes are like DMO and NMO but the operations occur in radial space. The analog to NMO is a simple time-invariant stretch hence the notation ω_s .

Unlike the constant-offset case, dip moveout is now done *before* the stretching, velocity-estimating step. Let us confirm that the dip moveout is truly velocity independent. Substitute (7) into the radial DMO transformation in table 2 to get the equation for transformation from time to stretched time.

$$\frac{h^2}{t^2} k_y^2 + \omega_s^2 = \omega^2 \quad (9)$$

We observe that the velocity v has dropped out of (9). Thus dip moveout in radial coordinates doesn't depend on velocity. Dip-moveout processing $\omega \rightarrow \omega_s$ does not require velocity knowledge. Radial coordinates offer the advantage that this comparatively costly process is done *before* the velocity is estimated $\omega_s \rightarrow \omega_0$.

The dip-moveout process, $\omega \rightarrow \omega_s$, is conveniently implemented with a Stolt-type algorithm using (9).

Although the foregoing analysis has assumed a constant velocity, we could revert to a $v(z)$ analysis after the dip moveout, just before conventional velocity analysis, stack, and zero-offset migration.

Both the radial-trace method and Hale's constant-offset method handle all angles exactly in a constant velocity medium, But neither method treats velocity stratification exactly nor is it clear that this can be done —since neither method is rooted in the DSR. Yilmaz (1979) rooted his DMO work in the DSR, so it can be expected to be exact for velocity stratification, but Yilmaz could not avoid angle dependent approximations. So there remains theoretical work to be done.

Anti-Alias Characteristic of Dip Moveout

You might think that if (y, h, t) -space is sampled along the y -axis at a sample interval Δy , then any final migrated section $P(y, z)$ would have a spatial resolution no better than Δy . This is not the case.

The basic principle at work here has been known since the time of Shannon. If a time function and its derivative are sampled at a time interval $2T$, they can both be fully reconstructed provided that the original bandwidth of the signal is lower than $1/2T$. More generally, if a signal is filtered with m independent filters, and these m signals are sampled at an interval mT , then the signal can be recovered.

Here is how this concept applies to seismic data. The basic signal is the earth model. The various filtered versions of it are the constant-offset sections. Further details can be found in a paper by Bolondi, Loinger, and Rocca (1982), who first pointed out the anti-alias properties of dip moveout.

EXERCISE

1. Describe the effect of the Jacobian in Hale's dip moveout process.